2
Literature Review

This chapter reviews the available literature for different areas of relevance with respect to the work reported in this thesis. The major topics reviewed for available literature includes: offshore structure, API pipeline steel and super duplex stainless steel materials, need of dissimilar welding, welding processes, development of shielded metal arc welding electrodes, and experimental investigations on dissimilar welds fabricated using GTAW process. The chapter also identifies the gap in the available literature, which has been further used to formulate the problem statement for this work.

2.1. OFFSHORE STRUCTURES

The offshore drilling activities of oil and natural gas are directly dependent on the global requirement. The year 2008 saw an unprecedented increase in the price of oil and gas [Hamilton J.D., 2009]. Hence a number of offshore drilling projects were started in this duration and successive years after it. There are various installations in the marine environment away from the shore, which are termed as offshore structures. These structures are used to drill oil and natural gas from ultra-deep wells and later on to transport the drilled product to refineries and distribution centers. The pipeline, also a variant of offshore structure, is then used to take the end product to different locations for consumption. Offshore structures are a hybrid of technical design, cost factor, and safety parameters. The last four decades have seen the growth of fixed platforms in three varieties: (i) steel template, pioneered in the Gulf of Mexico; (ii) concrete gravity type in the North Sea, and (iii) tension leg platform in Santa Barbara. Some of the important offshore structures are pipelines, platforms, drilling risers, compliant towers, jack-up drilling rigs, platforms, and support structures. Around 1891, the first submerged oil wells were drilled from a platform built on piles. Figure 2.1 represents different oil and gas offshore structures used in current times. The safety of offshore structures is very important. Offshore structures face a high rate of degradation and failure due to corrosion. Harsh environments promote corrosion and are more harmful to these structures. External factors such as the velocity of flowing water, pH, temperature, bio fueling, bacteria, composition, surface roughness, etc., cause significant loss to structure [Adumene, 2020]. An offshore structure needs to sustain harsher conditions in deep water locations located away from the shore, which makes the inspection and maintenance difficult and costly [Moghaddam et al., 2020]. There are many welded components in the spar type platform and foundations. These welded joints are most susceptible to failure because of corrosive water's combined action along with a cyclic load of wave and wind fluctuations [Larrosa et al., 2018].

The oil-gas exploration sector has always been regarded as a high-risk sector. The problem intensifies in offshore structures, where the human resource involved deals with the handling of hydrocarbons and oil and the harsh working environment [Bedaiko et al., 2010]. An offshore structure safety has two different challenges: personal safety and process safety [Swuste et al., 2016]. Personal safety hazards include exposure to hazardous substances at offshore sites, which leads to casualties or a severe blow to the health of working professionals involved [Mearns et al., 2006]. Process-related accidents include failure in structures, fire, explosions, spills, and other similar incidents. Process accidents are more hazardous and have far more wide-reaching consequences than the former [Knegtering et al., 2009]. The structural integrity of offshore structures is a direct measure of resistance to process-related accidents [Tang et al., 2018].

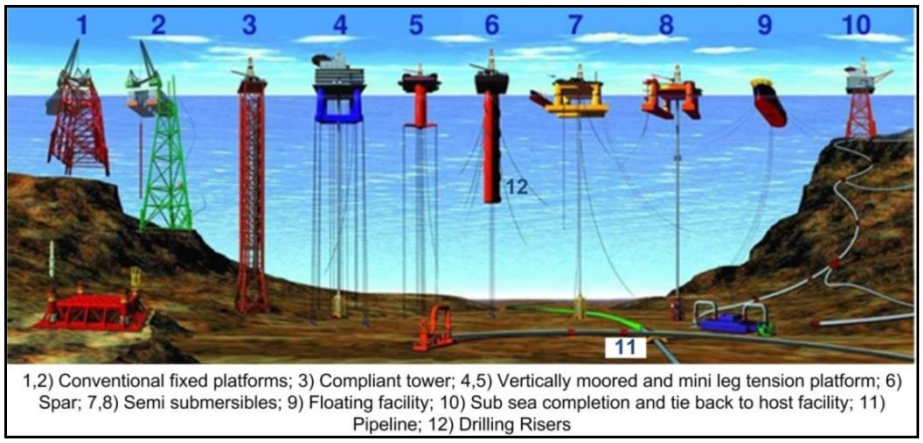

Figure 2.1: Types of offshore structures [Oil States Industries, Inc., 2008]

2.2. MATERIALS WITH OFFSHORE APPLICATIONS

Material for marine applications should possess high specific strength and corrosion resistance. The development of materials for a marine application is a demanding field and requires continuous research to provide materials with good properties and a combination of lightweight and durability [Rohith et al., 2019]. Marine-grade materials are expected to perform in varying and contrasting environments, such as sub-zero arctic regions, high-temperature equatorial regions, submerged underwater environments, to name a few. Broadly classifying a material with an offshore application is expected to have:

(i) Availability in different product forms (plates, pipe, tubes)
(ii) Easy and long availability
(iii) Economical
(iv) Good weldability
(v) Favourable strength to cost ratio
(vi) Effective corrosion resistance property

The choice of material depends upon the location of the application. Every component and location in an offshore site has different demands and requires a specific combination of properties to enhance the installation's structural integrity as a whole. Table 2.1 attempts to summarize the desirable properties from the material based on their site of application. Irrespective of location and type of component, the high corrosion resistance remains the most desired property. The marine splash zone is one of the most critical regions as it faces cyclic high-low tides, which cause wetting and drying cycles, accelerating the corrosion process. Figure 2.2 shows the different locations of an offshore structure.

Table 2.1: Marine location and property [Mvola et al., 2016]

S.No	Location	Property Required
1	Topside	High strength, Long service life, Excellent corrosion resistance
2	Splash Zone	Excellent corrosion resistance
3	Subsea	Low-temperature integrity, Excellent corrosion resistance

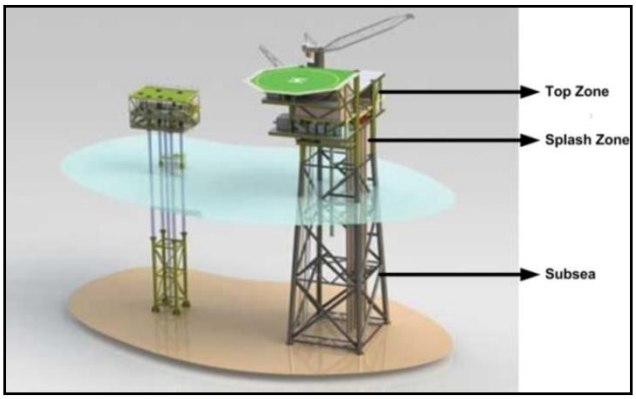

Figure 2.2: Different zones in offshore structures [Nicholson & Helle, 2013]

High strength low alloy steel is the most preferred material for marine applications [Huda et al. (2019a)]. They are widely used in oil-gas transportation and drilling risers because of good mechanical properties and corrosion resistance as compared to ordinary steel [Nathan et al., 2015]. These new grades of pipeline steel, which are basically low carbon micro-alloyed, consist of various micro-alloying components such as V, Ti, Nb, and a small amount of carbon and sulfur. For strain-based applications, HSLA steels should have sufficient toughness and deformability. Thermo mechanically controlled processing (TMCP), followed by accelerated cooling (ACC) promotes fine-grained microstructure by hindering dislocation mobility and gives the right combination of toughness and strength. The American Petroleum Industry (API) specifies most of the steel meant for pipeline applications. The first grade of steel produced solely for pipeline operations was designated as X42 in 1948. Where numerical designation 42 represented the yield strength of 42 ksi or 290 MPa in SI units. Since then several modifications have been made, and different grades were launched from time to time. Figure 2.3 represents the journey of development for various grades of pipeline steel in the last three decades, from the year 1990 onwards. There is no strict composition limits on the API pipeline steel, however comparative chemical composition for some of the recent grades from X70 to X120, based on available literature is summarized in Table 2.2

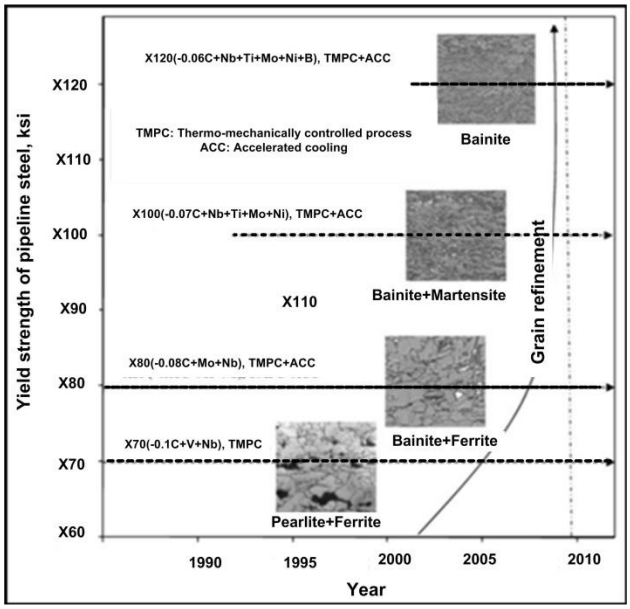

Figure 2.3: Development of different grades of pipeline steel from 1990 onwards [Liu et al., 2013]

Table 2.2: Chemical composition of API pipeline steel recent grades (%wt.) (Hillenbrand et al., 2004; Williams et al., 2006; Graf et al., 2004)

Grade/Element	X70	X80	X100	X120
Carbon	0.095	0.075	0.060	0.03-0.060
Silicon	0.32	0.31	0.35	0.36
Manganese	1.55	1.59	1.90	1.95
Phosphorus	0.015	0.018	not specified	not specified
Sulphur	0.001	0.001	not specified	not specified
Niobium	0.040	0.057	0.050	0.040
Titanium	0.013	0.013	0.018	0.020
Aluminium	0.030	0.026	not specified	not specified
Vanadium	0.060	not specified	not specified	not specified
Molybdenum	not specified	0.220	0.28	0.20
Niobium	not specified	not specified	0.25	not specified
Copper	not specified	not specified	not specified	not specified
Chromium	not specified	not specified	not specified	not specified
Boron (ppm)	2	not specified	not specified	10-20
Nitrogen (ppm)	52	60	40	40
Calcium (ppm)	8	11	not specified	not specified

One of the major reasons for updating the composition of pipeline steel is the demand for higher operating pressure, which has reached a value of approximately 80% in the present time. Later on, X52, X60 grades were developed, which has reached X70 being used extensively and most commonly in the current times. X80 grade has also marked its inception, whereas X100 and X120 are in the research and development process, going through numerous investigations for their commercial use expected to start in a few years. Microalloying has played an important role in the progressive development of API pipeline grade steels by imparting good yield strength, toughness, and good weldability. The microstructure is acicular ferrite-lower bainite rather than ferrite-pearlite, which leads to improvement in toughness. Also, the yield strength tends to remain at the same level after spiral pipe making [Das., 2010]. The pipeline steel is majorly produced using a basic oxygen furnace or an electric arc furnace. It is very important to take care of phosphorus content during the secondary refining process. The high presence of manganese in the final composition comes majorly from ferromanganese addition during the process. Ferromanganese also serves as a source of phosphorus. Hence the initial concentration of phosphorus during the primary process needs to be taken care of with utmost carefulness [Nara et al., 1981]. The pipeline steel is also made to undergo a vacuum unit to ensure low hydrogen and inclusion count. For sour applications like that of the sea environment, the sulphur content is desired to be kept below 10ppm. The pipeline steel at the site of the

application is expected to have the following qualities for their successful use: suitable mechanical properties, high weldability, low susceptibility to hydrogen-induced and sulphide stress cracking, internal soundness, and sound surface quality. The pipeline steel of API grades is hot-rolled at high temperatures. During this time, the steel has an austenite (ϒ) structure, and after exposure to high temperature, it is followed by rapid cooling. In the process of rapid cooling, the austenite partially transforms into pro eutectoid ferrite (α) and pearlite. This transformation occurring during cooling cycles results in microstructure to be a mix of pro eutectoid ferrite and pearlite. The pearlite in microstructure comprises pearlitic ferrite (α_p) and cementite (C_p) [Wang et al., 1999]. Observation of microstructure at low magnification reveals ferrite and pearlite rich bandings along the rolling direction. Dynamic recrystallization also plays an instrumental role in changing the morphology of the ferrite. As the cooling of hot rolled pipeline steel occurs, different kinds of ferrites are precipitated in the resultant microstructure. Polygonal ferrite (PF) is transformed at the highest temperature and slowest cooling rate. Another morphology of ferrite to be precipitated is Quasi Polygonal ferrite (QF), which is produced by transformation through short range diffusion across δ/ϒ interface. Granular bainitic ferrite (GF) is formed at the same transformation temperature as bainite, but at a slower cooling rate. Bainitic ferrite (BF) which is characterized with many elongated ferritic lath bundles with high density of dislocations separated with high angle grain boundaries; Acicular ferrite (AF) which is a complex structure consisting of QF, GF, BF and few PF with dispersed islands of second phases in the matrix it is characterized with relatively high density of dislocations. As the grades have progressed, the carbon percentage in composition has decreased further, which has led to the lowering of pearlite fraction. Pearlite appears in isolated and interlinked morphology, where the size of isolated pearlite particles was smaller than the interlinked ones. The most prominent site of isolated pearlite precipitation is the triple point or α/ α grain boundaries. High magnification observations also suggest the presence of finer carbides inside α grain. During ϒ to α transformation, ϒ rejects carbon, which is almost equal to the carbon concentration of the steel. If the diffusion of carbon is not fast, it will result in accumulation at the interface of ϒ/α interface, and subsequently, carbide precipitation will occur. Mintz et al., in their study, have presented a detailed discussion on precipitation of such carbides in pipeline steel [Mintz et al., 1989]. They have termed this precipitated carbide as gb carbide and have attributed their precipitation being directly related to the Mn content of the steel. As the grade of pipeline steel progressed, the Mn and carbon content decreased, and hence, the gb carbide precipitation was controlled. Once the significant transformation of ϒ to α has occurred, the remaining ϒ transforms to pearlite. Pearlite formation is majorly governed by the traditional mechanism of edgeways growth and sideways nucleation. After nucleation, the pearlite growth usually involves branching. A number of pearlite particle packets impinge on each other, and these packets have different orientations. Figure 2.4 represents the microstructure of typical pipeline steel of X52 grade.

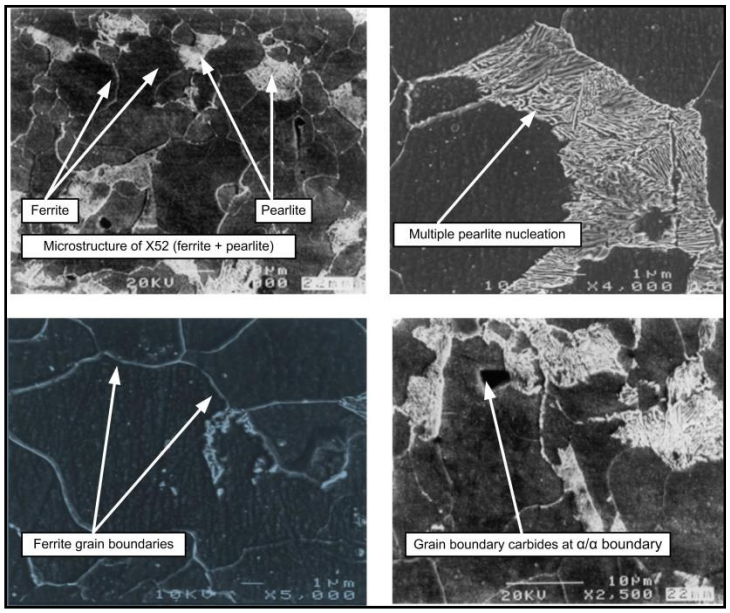

Figure 2.4: Microstructure of X52 pipeline steel [Wang et al., 1999]

The integrity and high reliability of pipelines depend upon multiple factors, such as external environment, fatigue, material defects, weld defects, internal and external corrosion, to name a few [Musa et al., 2015]. Due to prolonged exposure to the corrosive environment in offshore structures, the weld integrity of pipeline steel suffers. Hence, it is advisable to employ material with higher corrosion resistance in such locations. Nickel alloys are, without any doubt, the most suitable choice, but their application in such a large amount is ruled out due to its high cost.

Stainless steel with high chromium concentration is another option for employing in a corrosive marine environment. Steel having a chromium concentration of more than 10.5% by weight is referred to as stainless steel. Stainless steel can be classified into five major categories: ferritic, martensitic, austenitic, duplex, and precipitation hardenable. The difference in property of all these grades lies majorly in their microstructures. The most recent development in the grade of stainless steel is a duplex and super duplex stainless steel. The first grade of wrought duplex stainless steel is known to be produced in Sweden in 1930 for application in the sulphite paper industry [Armas, 2008]. The first known successful duplex grade developed specifically for enhanced protection against chloride stress corrosion cracking was 3RE60 [Newman, 2019]. The actual demand for duplex and its grades saw the first increase during the 1960s and 70s. During this period, an unprecedented shortage of nickel supply occurred, and a load of protection against corrosion increased tremendously upon austenitic stainless steel. Secondly, massive up-grading in the steel manufacturing industry due to the introduction of argon oxygen decarburizes practices occurred. Later in the 1980s, there was a second wave of development in the duplex steel when nitrogen addition resulted in improved weldability property of newly produced grade 2205 (22% chromium and 5% nickel). Duplex stainless steel performed exceptionally well in a corrosive environment, but the only drawback associated with it was its yield point limit of only 550 MPa. This issue could have been addressed with a cold-rolled finish, but that would have affected the sulfide stress corrosion cracking resistance adversely. Hence, this limitation was overcome by the development of a new grade super duplex stainless steel usually available in 2507 grade (25% chromium, 7% nickel), which is also referred to as SAF 2507 and UNS 32750 [Bergstrom et al., 2004].

Super duplex stainless steel has an enhanced yield limit of approximately 758 MPa. Pitting Resistance Equivalent Number (PREn) is often used to differentiate between the different grades of stainless steel. PREn is calculated using the empirical formula: %Cr + 3.3 %Mo + 1.65 %W + 16 %N [Charles, 1991]. The stainless steels with PREn below 30 are termed as a lean duplex, the one in the range of 30-40 is called duplex steel, whereas the grades having the value more than

40 are classified as super duplex [Bergstrom, 2007]. PREn values of different grades of stainless steel are provided in Table 2.3.

The duplex and super duplex stainless steel grade alloys contain chromium in the range of 20-30%, nickel 3-10%, molybdenum 0.5-7.5%, and copper 0-3% by weight. The concentration of carbon is kept low, usually below 0.4%. The alloy is quenched at a range of 1050°C to avoid precipitation of carbides and other intermetallic phases. The microstructure consists of a mixture of austenite and delta ferrite grains in almost equal proportionate (Figure 2.5). The balanced microstructure is achieved from the controlled addition of alloying elements. Each alloying element has its own role in strengthening a specified property, which establishes the supremacy of super duplex stainless steel. The addition of nitrogen has improved the weldability of this steel significantly. Similarly, the yield strength of dual phased duplex steel is twice the strength of single phased austenitic/ferritic steel. They also have improved toughness, ductility, intergranular, and stress corrosion resistance. These improved properties without much change in cost make them a suitable candidate material for application in the harsh marine environment. The super duplex stainless steel is now widely used in oil-gas, petrochemical, and paper-pulp industries. The super duplex stainless steel initially solidifies as δ ferrite, and as the cooling progresses, the precipitation of austenite occurs around 1200-1400°C at the grain boundaries. The alloy is also suited for welding operations such as butt and seam welded tubes. A high percentage of chromium in super duplex steel not only enhances its corrosion resistance but also implies good solubility of nitrogen. The presence of molybdenum improves the resistance to corrosion in chloride environments and also in reducing acids. Although a high amount of molybdenum with a high percentage of chromium increases the susceptibility of intermetallic precipitations. Nitrogen in super duplex steel plays multiple roles; it increases corrosion resistance and improves structural stability and austenite reformation after welding. Figure 2.6 represents the phase diagram for super duplex stainless steel as it solidifies with different proportion of austenite and ferrite.

Table 2.3: PRE_n values of different grades of stainless steel [Bergstrom, 2007]

Grade	UNS	C	Cr	Ni	Mo	W	Cu	N	PREn
Lean Duplex	S32101	0.03	21.5	1.5	0.3	-	-	0.22	25
	S32304	0.02	23	4	0.3	-	0.3	0.10	25
Standard Duplex	S31803	0.02	22	5.5	3.0	-	-	0.17	35
	S32205		22.5	5.8	3.2	-	-	0.17	36
Super Duplex	S32750	0.02	25	7	4.0	-	0.5	0.27	43
	S32760	0.03	25	7	3.5	0.6	0.5	0.25	42
Super Austenitic									
904L	N08904	0.02	20	24.5	4.2	-	1.5	0.05	35
254 SMO	S31254	0.02	20	18	6.1	-	0.7	0.20	43
Austenitic									
304L	S30400	0.02	18.2	8.1	0.3	-	-	0.07	20
316L	S21600	0.02	16.3	10.1	2.1	-	-	0.07	24

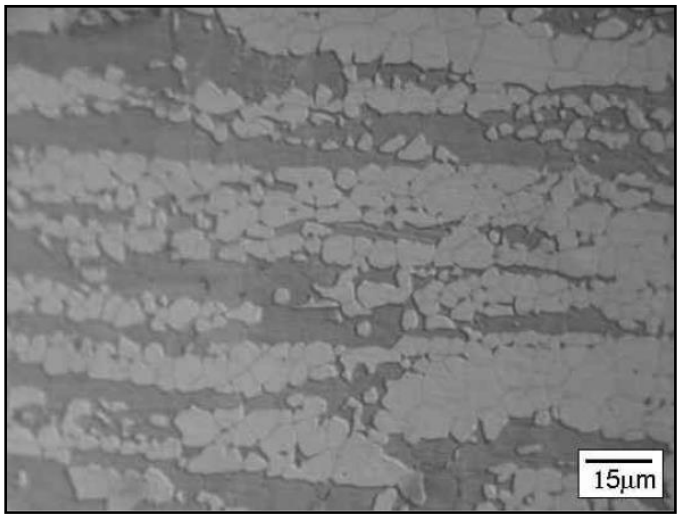

Figure 2.5: Microstructure of super duplex stainless steel [Armas, 2008]

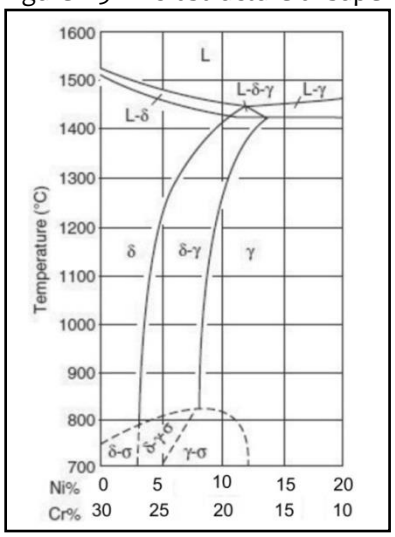

Figure 2.6: Phase diagram of super duplex stainless steel solidifying with different ϒ and δ proportion [Reick et al, 1990]

One of the major issues associated with super duplex stainless steel is the precipitation of intermetallic and secondary phases such as sigma, chi, R, and carbides due to exposure to high-temperature conditions. These phases are deleterious and affect various steel properties adversely [Nowacki et al., 2006; Labanowski et al., 2007; Niewielski et al., 2007; Topolska et al., 2009]. Embrittlement of super duplex stainless steel is yet another major issue that is dependent on multiple factors. In the case of steel with high carbon concentration, the presence of a carbide-forming network causes embrittlement phenomenon [Reick et al., 1990a]. Whereas for the low concentration steel, exposure to temperature range 475°C, the embrittlement is likely to occur. The embrittlement is caused due to precipitation of α' due to exposure at 475°C resulting in ferrite's embrittlement, embrittlement due to precipitation of σ phase in ferrite matrix [Pohl et al., 1990]. The interface energy of δ-δ and ϒ-ϒ boundary is higher as compared to the α-ϒ interface. Hence, during the hot working of steel, in the range of 900-1200°C, alternate ferrite and austenite lamellae microstructure is received. As solidification occurs, austenite and ferrite are almost equal in proportion. Exposure to high temperature in the temperature range below 1000°C significantly affects super duplex stainless steel's microstructure by causing precipitation of several intermetallic and secondary phases. The schematic TTT diagram for super duplex stainless steel, as represented in Figure 2.7, represents phase precipitation as a function of exposed temperature and its duration [Reick et al., 1990b]. The curve indicates that the high-temperature region indicated by C type curve presents the possibility of precipitation of sigma (σ), chi (χ), chromium nitride (Cr_2N), and carbides ($M_{23}C_6$) phases, whereas at the low

temperature range, embrittlement is likely to occur. These precipitate increase hardness, decreases ductility and toughness [Reick et al., 1998].

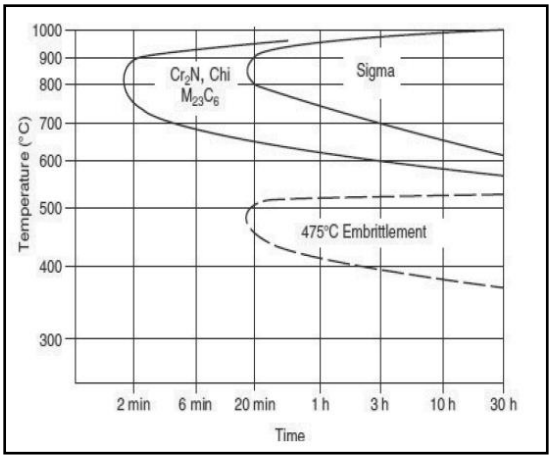

Figure 2.7: TTT diagram for super duplex stainless steel [Rosso et al., 2013]

α' is a cubic structure chromium-rich precipitate in the ferrite phase. It has a high coalescence resistance even upon exposure to temperature 350-450°C for a very long time duration. α' precipitation leads to cleavage fracture in the ferritic region, and its presence is difficult to trace even with very sophisticated transmission electron microscopy. Sigma is yet another intermetallic phase that has the potential to influence the property of super duplex significantly. It is hard and brittle in nature and is expected to contain chromium and molybdenum. The most rapid formation of sigma is seen upon exposure to temperature in the range of 700 to 900°C. A typical sigma phase nucleates in the ϒ-δ grain boundaries and further grows into adjacent δ. σ stabilizing elements such as chromium, molybdenum, and silicon increases the susceptibility of σ phase precipitation. Ferrite eutectoid decomposition (δ= σ+ϒ$_2$) is usually considered a driving force for the formation of the sigma phase in lamellar morphology, which is expected to be different at higher temperatures [Pardal et al., 2010]. Sigma and chi are both known to promote embrittlement of steel and are also referred to as deleterious phases [Nilsson et al., 2000]. Chi phase is regarded as a precursor of the sigma phase [Fonseca et al., 2017]. Sigma is also known to significantly influence wear and corrosion behavior, where the available literature reports that precipitation of the σ phase increases wear resistance, decreasing the pitting resistance characteristic. Kinetic of sigma phase formation has also been investigated by several researchers [Calliari et al., 2006; Escriba et al., 2009; Villanueva et al., 2006]. Most of the work reported on kinetics of sigma phase formation have uniformly excepted the theory proposed by Johnson and Mehl, Avrami, and Kolmogorov, which is referred to as JMAK or modified JMAK theory, and it mathematically represents sigma phase precipitation kinetics as shown in equation 2.1[Johnson et al., 1939; Avrami, 1939; Avrami, 1940; Avrami, 1941; Kolmogorov, 1937].

$$V_v = 1 - e^{-ktn} \quad (2.1)$$

Vv is the precipitated volume fraction of sigma, t is the time, k, and n are constants depending upon the nucleation rate, growth rate, and shape of the precipitate. The constant k is further calculated using equation 2.2.

$$k = k_o e^{-Q/RT} \quad (2.2)$$

Where Q is the activation energy for sigma phase formation, and R is the universal gas constant. The precipitation of these intermetallic phases causes the matrix's impoverishment in terms of alloying elements, chromium, nickel, and molybdenum, leading to deterioration in toughness and corrosion properties [Isern et al., 2016]. The microstructure of the sigma phase precipitated super duplex stainless steel after exposure to different etchant is shown in Figure 2.8.

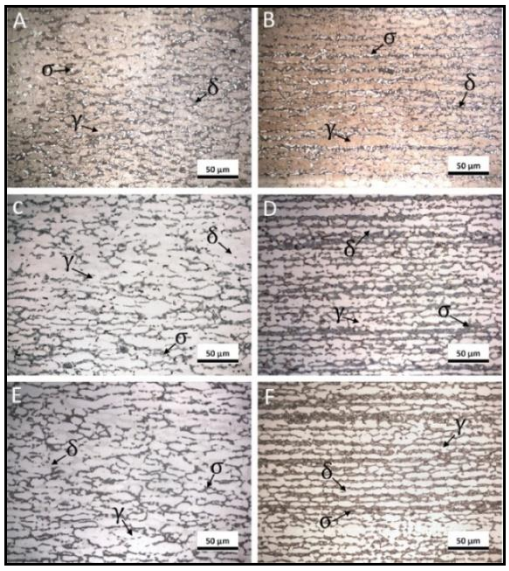

Figure 2.8: Microstructure of duplex and super duplex stainless steel after treating for 1 hour at 850°C: A, B- Glyceregia reagent, C,D- Grosbeck's reagent, E,F- Murakami (modified) reagent [Isern et al., 2016]

Hosseini et al. have reported that the temperature range of 630-1010°C witnesses almost 34% precipitation of σ phase [Hosseini et al., 2018]. As the aging temperature decreased from 1010°C to 640°C, the morphology of the σ phase changed from blocky to fine coral wood and an 80% decrease in thickness measurement. Sigma precipitation also witnessed the propagation of macro scale cracks, which was significantly larger in blocky morphology (Figure 2.9).

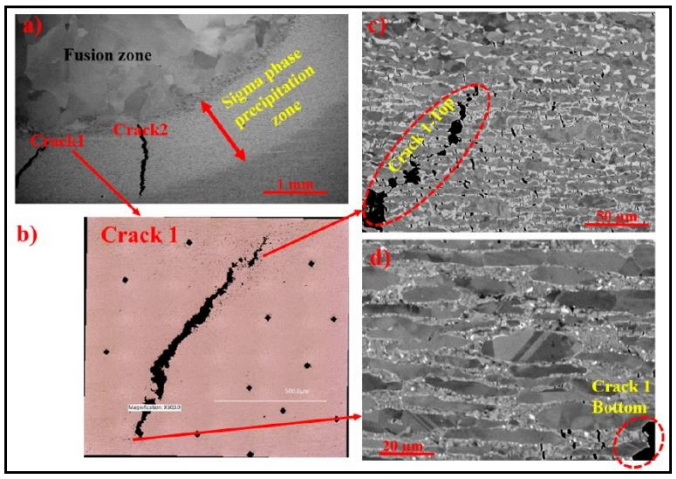

Figure 2.9: Sigma phase and cracks: (a) Two macro-scale cracks (b) Crack 1 surrounded by macro-scale cracks (c) Blocky σ with cracks (d) Coral σ with cracks [Hosseini et al., 2018]

The pitting corrosion resistance was also found to be dependent upon aging temperature and consequent sigma phase morphology [Hosseini et al., 2018]. Figure 2.10 represents the EBSD, and inverse pole figure (IPF) maps of σ precipitation at different temperatures along with a transformation in morphology from blocky to coral shaped as the aging temperature was reduced. Similarly, Fargas et al. have reported an increasing effect of sigma phase precipitation on wear resistance of super duplex stainless steel, in which they have concluded precipitation of around 40% after heat treatment of three hours at 875°C [Fargas et al., 2013]. Similarly, other studies have also been conducted where the effect of sigma phase has been reported on different performance characteristics of super duplex stainless steel [Shockley et al., 2017; Meng et al., 2007; Angelini et al., 2004; Potgeiter, 1999]

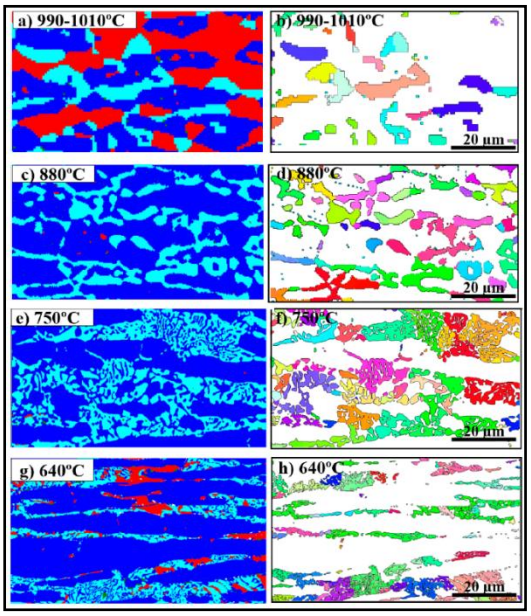

Figure 2.10: EBSD (a, c, e, g) and Inverse Pole Figure (IPF) maps (b, d, f, h) of σ precipitation at different temperatures along with the change in morphology from blocky to coral shaped [Hosseini et al., 2018]

2.3. WELDING OF OFFSHORE COMPONENTS

This section deals with similar metal welding of pipeline steel and super duplex stainless steel. The issues related to these welds have been discussed, along with the need for dissimilar joint between super duplex stainless steel and pipeline steel has been mentioned.

2.3.1. WELDING OF PIPELINE STEEL

High strength low alloy API grade pipelines steels find excessive application in offshore structures. Their properties and applications have been discussed in detail in the previous section 2.2. The offshore structures are available in a different range of sizes and require successive joining. Oil-gas transportation pipelines stretch over thousands of kilometers, whereas the drilling riser's length varies with the well's changing depth from the offshore platform. The weldability of pipeline steel is dependent upon carbon equivalent (CE), which is a measure of its hardenability and crack susceptibility. CE helps correlate and assess the effect of alloying elements on the microstructure of welded pipeline steel, which is directly related to its mechanical properties. American Petroleum Association (API) uses two different formulae (CE_{IIW} and CEP_{CM}) for computing the carbon equivalent of pipeline steel and its weld [Sharma et al., 2017]. The two proposed formulae are used based on the weld zone's carbon concentration specified by the American Petroleum Association [American Petroleum Association, 2012]. CEP_{CM} includes critical metal parameters and covers more elements as compared to the equation adopted by IIW. These two formulae are represented by equations 2.3 and 2.4 [Ito and Bessyo, 1968]:

$$CEP_{CM} = \%C + \frac{\%Si}{30} + \frac{\%Mn+\%Cu+\%Cr}{20} + \frac{\%Ni}{60} + \frac{\%MO}{15} + \frac{\%V}{10} + 5\%B \quad \text{(if C} \leq 0.12\% \text{ by weight)} \quad (2.3)$$

$$CE_{IIW} = \%C + \frac{\%Mn}{6} + \frac{\%Mo+\%V+\%Cr}{5} + \frac{\%Cu+\%Ni}{15} \quad \text{(if C} > 0.12\% \text{ by weight)} \quad (2.4)$$

Apart from chemical composition, the thermal cycles, heat input, and cooling rate also significantly influence the weld microstructure. The mentioned factors and resultant property in microstructure are majorly driven by the welding process. Pipeline weld joints are fabricated using numerous welding processes, including both the conventional arc welding and non-conventional methods (Table 2.4). Pipeline steels can be welded either using filler metal (SAW, GMAW, SMAW, GTAW) or without filler metal (Continuous, electric, and laser welding). API 1104 code specifically deals with the welding of pipeline and related facilities, including the repair work [American Petroleum Institute, 2005].

Table 2.4: Welding processes used for welding pipeline steels [API, 2005]

Welding Process	API pipeline steel-grades		
	X42 to X70	X80	X90 to X120
Without filler metal			
Electric Weld	√	√	
Laser Weld	√		
With filler metal			
Submerged arc weld	√	√	√
Gas metal arc weld	√	√	
Combined GMAW+SMAW	√	√	

Literature reveals significant work has been done to fabricate welds with non-conventional processes that have no filler metal involvement. Friction stir welding has been widely used for welding pipeline steels. Fabrication of friction stir weld of API X80 steel and characterizing it for impact energy at various sub-zero temperatures ranging till -40°C indicate the suitability of the FSW joint of X80 at -20°C, as it possesses significantly high impact value [Avila et al., 2015]. High-pressure hydrogen assisted fatigue crack growth behavior was investigated for friction stir welded X52 pipeline steel. Tests were performed on base metal, weld center, and 15mm away from the weld. The hydrogen assisted crack growth was found to be moderately high for the weld zone compared to the base metal. Even the fatigue crack growth rate relationship was found comparable to the conventionally arc welded pipeline steel joints [Ronevich et al., 2017]. Microstructure investigation of multi-pass friction stir welded X80 steel plates indicate that the weld zone consists of granular bainite and bainite packets with irregular and straight ferrite plates. It has also been reported that friction stir weld is a better process for joining pipeline steel than conventional arc welding methods. Due to lower peak temperatures in the former, they are less prone to austenite and martensitic band growth [Avila et al., 2016]. Some available studies have attempted to correlate the FSW parameters with microstructural features, such as material flow, texture, reconstruction of prior austenite grain boundaries, and residual stress [Young et al., 2013; Abbasi et al., 2012; Steuwer et al., 2012]. Similarly, several studies are available, whereas extensive characterization of friction stir weld of pipeline steel has been experimentally characterized for various properties, aiming to establish its acceptability as a prospective joining process [Santos et al., 2010; Kumar et al., 2010; Sowards et al., 2015]. A limited attempt has also been made to fabricate discussed weld with other non-conventional processes such as hybrid laser arc welding [Gook et al., 2014; Miranda et al., 2010; Moore et al., 2004]. Laser hybrid welds on grades up to X70 have demonstrated high impact toughness with a maximum wall thickness of 16mm, whereas for X80 grade onwards, the results are pretty much acceptable with a root face depth of 9mm [Vollertsen et al., 2010; House et al., 2005]. Conventional arc welding methods are widely used for original part fabrication and repair, maintenance activities. Since most of the repair work of offshore structures is conducted onsite, hence conventional processes are more preferred due to their easy setup and flexibility. Submerged arc, shielded metal arc and gas metal arc welding process are the most preferred processes. Experimental characterization of submerged arc welded X65 pipeline steels reveals the welding process, and chosen parameters majorly influence the microstructure, chemistry, and properties of HAZ. With an increase in cooling temperature, the microstructure becomes finer, and its tensile and

impacts strength increases [Chen et al., 2014]. Hashemi et al. have fabricated double submerged arc weld of X65 line pipe steel and investigated the hardness and impact toughness in different weldments zones [Hashemi et al., 2012]. The results conclude that due to the cast microstructure and grain boundary phases such as pro eutectoid ferrite, the fusion zone had low impact energy and high hardness value.

2.3.2. WELDING OF SUPER DUPLEX STAINLESS STEEL

Duplex and super duplex stainless steel welds find numerous applications in offshore applications. These joints, with excellent corrosion resistance and superior mechanical properties, enhance the integrity of the structure significantly. The balanced ϒ/δ ratio of duplex stainless steel is termed as the main reason for its superior properties. But achieving the same in its weld is a challenging task. The duplex and super duplex stainless steel are welded using different arc and solid-state welding processes. Conventional arc welding processes such as GTAW, GMAW, SMAW, FCAW, SAW have high arc energy, and they promote a higher amount of austenite precipitation in the weld zone [Kannan et al., 2006; Nowacki, 2009]. Processes such as plasma arc welding (PAW), laser beam welding (LBW), and electron beam welding (EBW) have a faster cooling rate and cause a fewer amount of austenite in the weld. Apart from these processes, advanced joining techniques such as friction stir welding (FSW), activated TIG (A-TIG) hybrid plasma GMAW/GTAW, is also widely used in fabricating duplex/super duplex weld [Rai et al., 2011; Theodoro et al., 2015]. Figure 2.11 represents macrograph and microstructure for different welding processes. The weld and HAZ microstructure is significantly influenced by the process, welding consumable, parameters, and thermal cycle [Murugan et al., 1998]. The super duplex weld's heat-affected zone is divided into two narrow zones: High-temperature heat affected zone (HT-HAZ) and Low-temperature heat affected zone (LT-HAZ). The HT-HAZ is situated just next to the fusion boundary and is often characterized by the higher ferrite fraction and presence of nitride particles [Liao, 2001; Tao et al., 2015]. Whereas the LT-HAZ is situated next to the base metal and witnesses the precipitation of intermetallics such as sigma and chi [Wang, 2005; Nishimoto, 2006]. The weld zone microstructure is multiple austenites in the ferrite matrix, mainly due to the melting and solidification of filler metal. The microstructure of the weld zone differs significantly from base metal along with a considerable difference in alloying element distribution [Westin et al., 2014]. The main factors which control the super duplex weld microstructure are filler metal, shielding gas, dilution, and element loss during the welding process [Hosseini et al., 2020]. Usually, overmatching fillers are preferred for welding super duplex steel. These fillers have a high amount of nickel to promote austenite formation [Kotecki, 1986]. Nitrogen-containing shielding gas is also preferred to promote austenite formation in the weld zone microstructure [Karlsson, 2012]. Figure 2.12 below represents the microstructure map of a super duplex stainless steel weld. Computational thermodynamics is a strong tool which has been used by researchers to predict the precipitation of austenite in weld zone, microstructure coarsening, precipitation of secondary phases and pitting corrosion resistance equivalent number, and critical pitting temperature [Tan et al., 2009; Wessman et al., 2010; Wessman et al., 2013, Wessman et al., 2014]. As per industry standards, the austenite concentration less than 25-30 % in the weld zone is not acceptable for practical applications [Hsieh et al., 2001; Norsok Standard, 2004]. Heat input also plays a significant role in influencing the quality of duplex/super duplex steel welds. For the SMAW process, the weld fabricated with heat input in the range of 2.5-4 kJ/mm, showed an increase of tensile strength up to 3 kJ/mm and decrease after that, whereas impact strength of weld decreases with the increasing heat input, thereby suggesting 3 kJ/mm as the optimum value [Nowacki et al., 2005]. For the GTAW process, the increasing heat input has been found to have a favorable impact on the pitting corrosion resistance of the weld [Ume et al., 1987]. Post weld heat treatment of duplex weld fabricated using SAW at 650°C for 0.5 hours causes dissolution of σ phase in the weld zone, whereas the welds without PWHT had significant

precipitation of σ in the weld zone and around fusion line due to segregation of alloying elements [Luo et al., 2014].

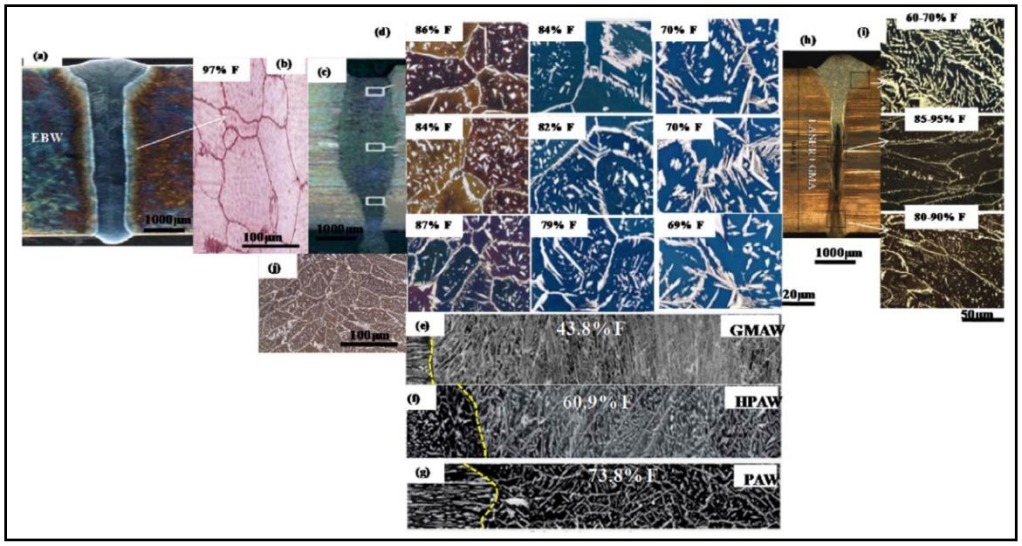

Figure 2.11: Weld microstructure obtained from different welding processes: (a) Weld bead EBW (b) Microstructure EBW (c) Hybrid weld bead (d) Microstructure with different cooling rate and ferrite content (e) GMAW weld (f) Hybrid PAW weld (g) PAW weld (h) Hybrid (laser + GMA) weld bead (i) Weld microstructure at different sections (j) Hybrid (laser+MIG) weld [Verma et al., 2017]

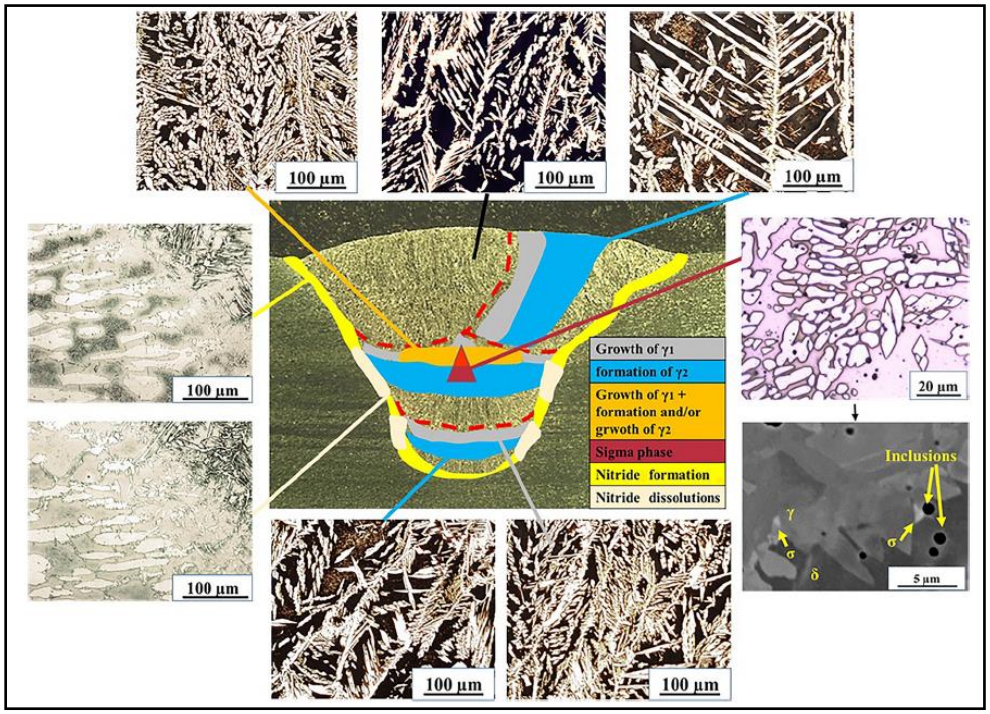

Figure 2.12: Microstructure of multi pass super duplex stainless weld [Hosseini et al., 2020]

2.3.3. NEED FOR DISSIMILAR WELDING OF PIPELINE/SUPER DUPLEX STAINLESS STEEL

Pipeline steel extensively used for offshore applications suffers a great loss due to continuous exposure to a corrosive environment. Higher corrosion-resistant alloys have been developed, but they cannot completely replace the HSLA pipeline steel due to economic factors and other required properties associated with the system. This problem increases in critical locations such as the marine splash zone for drilling riser and branching point of transportation pipeline,

where the stress concentration factor increases considerably. Mexican Petroleum Industry (MPI) has been using two solutions (Figure 2.13) to take of this issue in offshore sites: (i) carbon steel sleeve, (ii) cathodic protection [Mendoza et al., 2010]. Though these methods gave good results, they require permanent maintenance and inspection. Hence another prospective solution is substituting the pipeline steel in such location with super duplex stainless steel. A Kela-2 gas field in China runs for almost 4000 km and is one of the leading natural gas supplies. Here, duplex stainless steel has been used between the gathering and mainline by joining the API X80 pipeline steel for around 13 km [Wang et al., 2009].

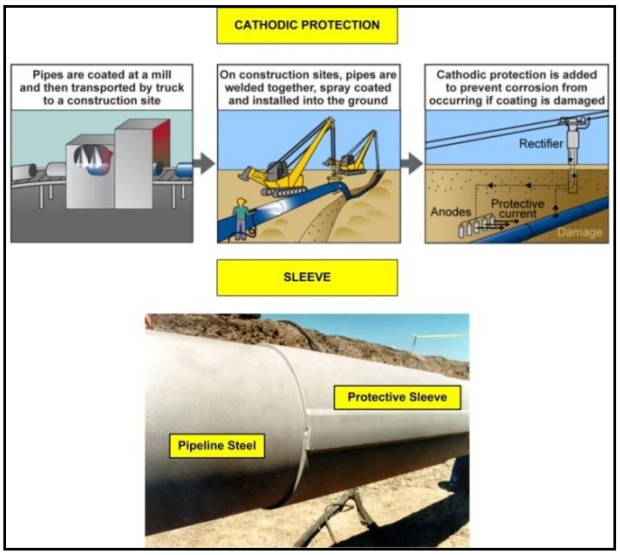

Figure 2.13: Protection methods suggested by MPI [GAO 17-639]

Pipelines, process piping, and process vessels are usually made up of carbon steel, stainless steel, nickel alloys, and duplex steel. The operating environment plays an important role in deciding the particular material. Usually, high corrosion resistant-cost effective duplex steel is welded to the pipeline steel in the critical regions such as marine splash zone, branching and sub branching points of distribution network for prolonging the life of the structure. The large distance pipeline usually witnesses a number of such dissimilar joints. Whereas, in the pressure vessels, the nickel alloys are now increasingly joined with duplex grade.

2.4. DESIGN & DEVELOPMENT OF SMAW ELECTRODE COATING

Shielded metal arc welding (SMAW) is one of the most versatile processes used in the fabrication of nearly all offshore structures. It is widely used for joining similar/dissimilar metals, repairing, and maintenance operations. Coated electrodes used in the SMAW process influence the weld integrity significantly. The coating protects the molten weld pool from the ambient impurities by forming protective slag covering and serves as a source of alloying elements in the weld zone. Flux used in submerged arc welding (SAW) and coated electrodes in SMAW processes have a somewhat similar role in refining the weld performance. Their basicity index often markets the coated electrodes for the SMAW process, and very limited information about actual composition is available in the open domain. Due to this, a few organizations involved in developing electrodes have always monopolized the market. This leaves end-users with a limited choice of competing options to select the most suitable electrode for their application area. This section discusses the SMAW process, the effect of coating composition on weld, various approaches in practice for designing and developing the SMAW electrode coating compositions, and different approaches for coating characterization.

2.4.1. SHIELDED METAL ARC WELDING (SMAW) PROCESS

The SMAW is also referred to as manual metal arc welding (MMAW) and is one of the most widely used welding processes. With the advent of the advanced joining process, a shift from its usage is being witnessed, but its superiority is maintained for short-run and repair activities. Small workstation and ease of use make it one of the most versatile and user-friendly process. The process employs a filler core wire coated with mineral compositions; it is connected to the power source from where electric current is supplied, which is used to initiate arc in between the electrode and workpiece to be welded. The electrode is brought in close contact with the metal to initiate the arc and then pulled away backward. With the heat of the arc, the filler metal melts and gets deposited on the desired place of the workpiece. Also, along with filler, the melting of the electrode coating occurs, which decomposes to releases gas to protect the molten weld pool and add alloying elements. This coating further solidifies and forms a protective slag covering around the molten pool to protect it from impurities. This slag covering is then chipped off to obtain a finished weld surface. Electrode coating can be either cellulosic, rutile, acidic, or basic in nature, depending upon its composition. A representative image of the SMAW process is shown in Figure 2.14.

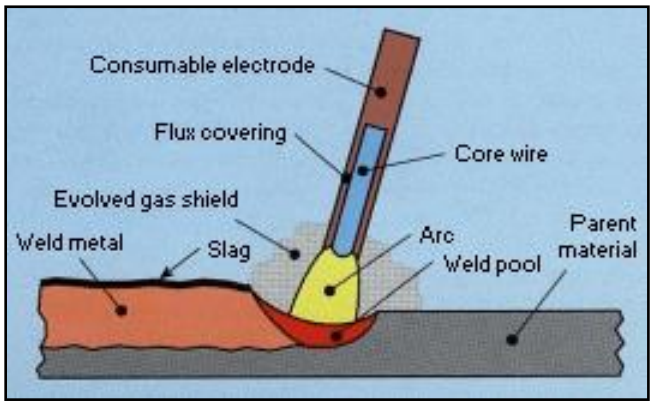

Figure 2.14: Representation of the SMAW process [TWI-MMAW]

2.4.2. NATURE AND ROLE OF COATING CONSTITUENTS

The electrode coating comprises different minerals, each having its role, along with interactions products obtained with other minerals. Some of the commonly used minerals are calcite, fluorspar, silica, rutile, calcinated bauxite, deadly burnt magnetite. Various functions performed by these minerals and their interactions are slag former, deoxidizers, arc stabilizers, binding agents, desulfurizing agents, etc. to name a few (Table 2.5). Obtaining a sound weld requires a stable arc, sufficient slag formers, binding agents, and micro alloying elements to improve specific properties based on the application site. Elements acting as arc stabilizers are added to enhance the arc stability, whereas slag formers are added to increase the slag formation, which in turn protects the molten weld pool from the ambient impurities. Binding agents are an essential part of the composition as they hold together different minerals in the coating so that they can perform as a single unit. Slipping agents are added in a controlled quantity to ease up the extrusion of coating on the core filler wire. Several gas-forming elements are added to take the unwanted, deleterious elements from the weld pool during the gas-metal and slag metal reactions [Bhandari et al., 2016a]. These gas-forming elements significantly reduce porosity defects in welds [Bhandari et al., 2016b]. The role of different minerals in SAW fluxes and SMAW coatings has been discussed in detail by the previous researchers [Mahajan et al., 2019; Sharma et al., 2020; Sharma et al., 2019]. It is essential to add these minerals in suitable amounts to ensure that they perform satisfactorily and contribute to weld performance's intended objective.

Table 2.5: Role of electrode coating constituent minerals [Mahajan et al., 2019; Sharma et al., 2019]

S. No	Mineral	Chemical Formulae	Role
1	Talc	$2MgO.4SiO_2.4H_2O$	Slag former, slipping agent
2	Calcium Carbonate	$CaCO_3$	Shielding gas, fluxing agent
3	Fluorspar	CaF_2	Slag former, fluxing agent
4	Cellulose	$(C_6H_{10}O_5)_x$	Shielding gas, deoxidizer
5	Feldspar	$K_2O.Al_2O_3.6SiO_2$	Slag former. Arc stabilizer
6	Silica	SiO_2	Slag former. Arc stabilizer
7	Potassium Silicate	$K_2SiO_3.nH_2O$	Arc stabilizer, binding agent
8	Mica	$KAl_2(OH)_2$	Extrudability, arc stabilizer
9	Sodium Silicate	$Na_2SiO_3.nH_2O$	Slag former, arc stabilizer
10	Manganese Powder		Slag former, alloying element
11	Ferroalloy Powder		Deoxidizer

2.4.3. EFFECT OF COATING CONSTITUENTS ON WELD

Physicochemical, thermo physical and structural properties of flux depend on its constituents and influence the welding property significantly. Coating constituent minerals interact with each other through gas-metal and slag-metal reactions at the interface of the molten weld pool. These reactions lead to the formation of complex chemical compounds. The viscosity of molten coating is very important as it ensures proper penetration and ensures that the slag formed in the end covers the bead completely [Mitra et al., 1991a; Kalisz et al., 2013]. Calcite in the coating mixture reacts with silica to form a complex silicate ion known as a good network former. This silicate ion in the system increases the density of molten flux and slag. The addition of manganese oxide (MnO) along with fluorspar (CaF_2) is known to act as a network breaking agent for silicate ion, which lowers its viscosity and hence has a positive impact on the flowability of molten flux and slag [Olson et al., 1998; Roy et al., 1954; Mills, 2011; Bhandari et al., 2016b]. Rutile is yet another important constituent of electrode coating known to have a synergistic effect on the slag detachability. An increase in the amount of acidic minerals such as silica, alumina, and corundum increases the slag detachability. An increased amount of CaF_2 results in the formation of the cuspidine phase in slag. Cuspidine, along with the formation of the cordierite phase, lowers the slag detachability (Bhandari et al., 2016a, 2016b). Arc stability has a significant impact on weld quality. The lesser the spatter in an arc, the more sound profile bead is obtained. Discontinuous arc results in improper deposition of filler wire, and the fabricated weld has multiple defects [Patchet, 1974; Niaga, 2002; Suban, 2003]. Potassium silicate, sodium silicate, calcite, and rutile are known to improve arc stability by enhancing electrical conductivity [Natalie et al., 1986]. CaF_2, on the contrary, is known to reduce the arc stability [Witting, 1980; Rissone et al., 1997; Farias et al., 1997; Olson et al., 1998]. The oxygen content of the weld influences its performance significantly. Specifically, in marine applications, weld's oxygen content has a deciding role to play when it comes to weld qualification for the actual application. Oxygen in the weld increases the inclusions and affects the element transfer efficiency from the electrode tip to the molten pool. Some oxides present in coating disassociate due to the high heat of the arc and form various oxides. FeO, MnO, SiO_2 have been predicted to increase the oxygen content of weld. The thermal stability of oxide, along with solidification time, plays an instrumental role in influencing the weld's oxygen content. Mitra et al., have proposed a kinetic model for element transfer from the electrode to the weld pool [Mitra et al., 1984]. The chemical interaction between weld and slag can be divided into three stages, which

occur within: (i) droplet, (ii) weld pool, (iii) solidified weld pool [Mitra et al., 1991a; Mitra et al., 1991b]. Literature reveals the presence of various studies on the role of flux on mechanical and metallurgical properties of the weld [Chen et al., 1989; Fox et al., 1996; Mercado et al., 2005; Jindal et al., 2013a; Jindal et al., 2013b; Jindal et al., 2014; Polar et al., 1991]. CaO-CaF_2-TiO_2 based SMAW electrode coatings were developed for hard-facing applications, too, and the results have indicated that CaF_2 in the coating composition increases the deposition rate [Cruspo et al., 2010]. Nickel offers good mechanical properties to weld joints in offshore and high-temperature applications. $CaCO_3$-Na_2CO_3-CaF_2 based coating and the addition of different ferroalloys (Fe-Nb, Fe-Ti, Fe-Si) were extruded on the nickel-based core wire, and experimental results showed that the addition of specific ferroalloy increased that particular alloying element's concentration in the weld zone [Qin et al., 2013]. Similarly, nickel-based electrodes were also prepared using Na_3AlF_6, TiO_2, and $CaCO_3$ mineral constituents for power plant applications, where cryolite was added in a suitable amount for enhancing the weld cleanliness [Sham et al., 2014]. Very limited literature is available on the design and development of SMAW electrode coating compositions for marine applications. Atia et al. have developed rutile-based coatings for extrusion on duplex 2205 core wire. The basicity index of developed composition was kept at three levels of 1.1, 1.2, and 1.4. They concluded that an increase in the basicity index of coating composition reduces the weld impurity level. An extensive investigation of the microstructure of the weld zone was also conducted, which has been closely related to the cooling rate of the weld and its mechanical properties [Atia et al., 2020]. Osio et al. have developed welding consumables for offshore joints with particular emphasis on controlling porosity and precipitation of acicular ferrite in the weld fusion zone. They concluded that the addition of ferrotitanium (Fe-Ti) in the coating composition increases the silicon and manganese in the weld, which in turn increases the hardenability. Another interesting observation derived from this study was optimum 12.5 wt.% presence of $CaCO_3$ was found to reduce the porosity, whereas a further increase in its concentration leads to an unstable arc and poor slag detachability. A correlation between coating composition and weld metal chemistry, hardness has been drawn in this study, which is represented in Figure 2.14. Significant work has been reported for SMAW electrode development for thermal, nuclear power plant applications. The limited literature availability clearly represents a void of investigations in the field of SMAW consumable development for a specific application in offshore marine applications that required attention to ensure competitive product availability to enhance the structural integrity of offshore structures.

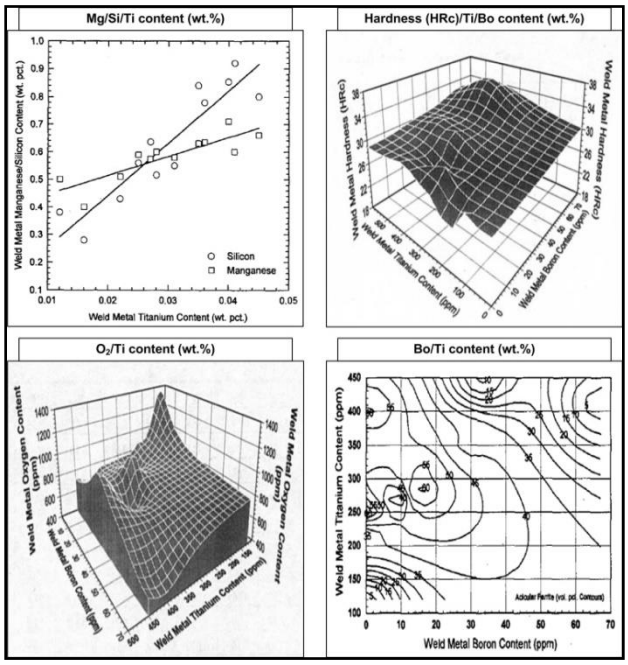

Figure 2.15: Weld metal chemistry and properties [Osio et al., 1995]

2.5. GAS TUNGSTEN ARC WELD (GTAW) FOR OFFSHORE APPLICATIONS

This section discusses the basic principle of the GTAW process, highlights its application in fabricating welds for offshore application, and mentions various experimental characterizations of dissimilar welds of duplex/super duplex stainless steel/API pipeline steel along with some other joints.

2.5.1. GTAW PROCESS

Gas tungsten arc welding (GTAW) process, also known as Tungsten inert gas (TIG) welding process, uses a non-consumable tungsten electrode to weld materials. The arc is created between the tungsten electrode and metal to be welded, whereas the filler metal is fed from an external source, mostly in the form of a bare-metal filler rod [Smith, 2007]. Tungsten is preferred for electrode material as it has a high melting point of around 3410°C. The arc melts the filler metal and is added to the weld pool. A schematic diagram of the GTAW process is shown in Figure 2.15. GTAW is comparatively slower than other methods but has a better surface finish and requires little or no finishing operation, as there is no spatter [Mallick et al., 2010].

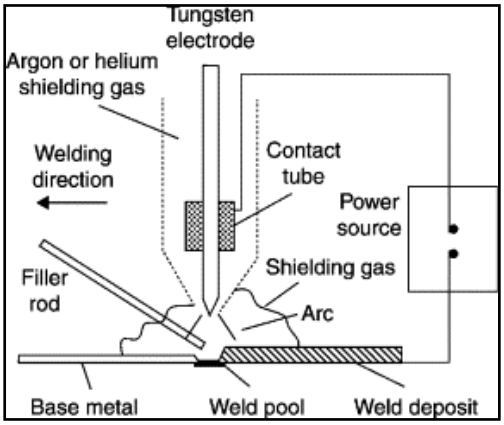

Figure 2.16: Schematic representation of the GTAW process [Tejedor et al., 2013]

GTAW can be conducted either using direct current (DC) or alternating current (AC). Tungsten electrode connected to the positive makes the mode direct current electrode positive (DCEP), whereas upon connected to negative, it is termed as direct current electrode negative (DCEN). In the DCEN mode, 70% of the heat is generated at the anode, which is the workpiece, and 30% at the cathode, which is the electrode. DCEN mode has higher heat input associated with it, which causes deeper penetration as compared to DCEP mode. In the DCEP mode, a higher heat generation is observed at the electrode holder, which requires an external cooling, most preferably in the form of water-assisted cooling. A large stream of positive ions strikes the workpiece in DCEP mode, which makes the surface cleaner and removes the pre-formed oxide layer; this is termed as cathodic cleaning action [Lathabai, 2011]. GTAW process can be either used alone or in combination with other welding processes. In some cases, it is used to give the root pass, whereas further passes for filling of grooves are done using SMAW, FCAW, and GMAW, etc. GTAW provides good process control and desirable dilution of approximately 30%, keeping the weld properties almost in the range of base metal. Shielding gases are also an important tool for controlling weld quality in the GTAW process. Using pure argon gas for super duplex stainless steel welds can lead to nitrogen loss, whereas the inclusion of nitrogen in the gas mixture can significantly increase the weld nitrogen component beyond the desirable range. Increased nitrogen can lead to weld metal porosity, spitting, and sparking of the weld pool, along with the potential to alter the solidification mode. Helium is also suggested to be an important shielding gas. Helium produces a hotter arc through an increase in the arc voltage. Helium (He) in the shield can lead to a rise in the travel speed in proportion to the rise in voltage. However, too much He can make the pool challenging to control. Similarly,

hydrogen additions to the shielding gas enhance the arc voltage and can be used to increase travel speed for the same arc energy as pure argon (Ar). The use of Ar+3%H_2 should be treated with extreme caution, as it has the possibility of increased susceptibility to hydrogen cracking of weld [Gunn, 1997].

2.5.2. FABRICATION AND CHARACTERIZATION OF DISSIMILAR OFFSHORE WELDS USING GTAW PROCESS

This section discusses the fabrication and experimental characterization of dissimilar metal welds with offshore applications fabricated using the GTAW process. The discussion focuses upon solidification mode, weld fabrication, metallurgical and mechanical investigations carried out by previous researchers.

2.5.2.1. SELECTION OF CONSUMABLE FOR GTAW PROCESS FOR SUPER DUPLEX STAINLESS STEEL

Selection of a suitable consumable in the GTAW process plays an important role in ensuring correct solidification mode, achieving desirable phase balance, avoiding solidification cracking, and enhancing mechanical properties [Wahid et al., 1993]. Super duplex stainless steel prefers the use of an overmatching consumable. The filler metal should have around 2-4% higher Ni as compared to the base metal, which promotes austenite formation to make up for the loss, which occurs during cooling of the weld. However, the literature reveals that researchers have different views regarding over alloyed Ni filler usage. Some have advocated using over alloyed high Ni filler, which would impart superior corrosion resistant properties, whereas few others have suggested that Ni can accelerate the precipitation of intermetallic in the weld fusion zone [Liljas, 1984; Gooch, 1996]. Due to the high nickel cost, a balanced approach is more suitable for developing and using filler to fabricate super duplex weld. The resultant microstructure of the weld zone has an important say in final properties. Hence, it is essential to know the microstructure that particular filler would yield upon solidification and further cooling down. The chemical composition and behavior of super duplex steel and pipeline steel are entirely different; hence, it is impossible to use filler that would match both the metals. There are different constitutional diagram available which can be used to predict the weld microstructure. The most important constitutional diagrams which are being used for this purpose are Schaeffler, Delong, and WRC-1992 [Kotecki et al., 1992]. Figure 2.16 shows all three diagrams. WRC-1992 includes a separate term for nitrogen content while calculating Ni_{eq}; it is most preferred for the duplex/super duplex steels [Verma et al., 2017].

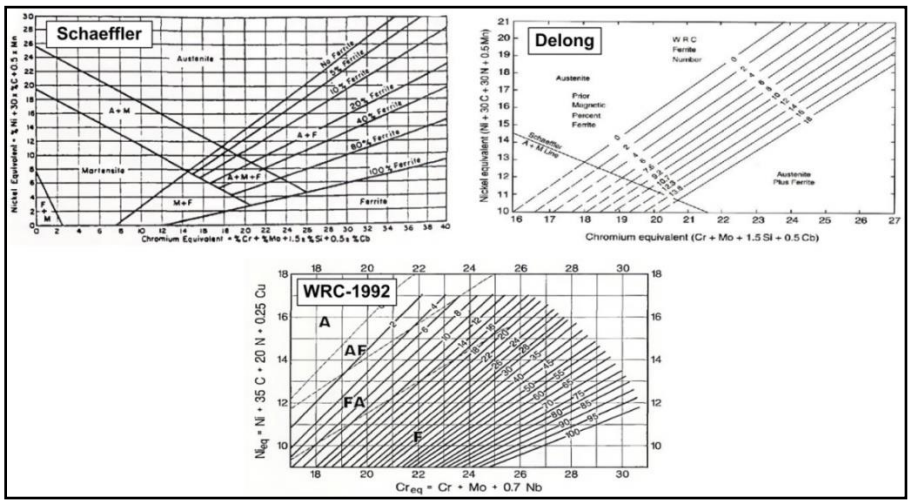

Figure 2.17: Constitutional diagrams [Verma et al., 2017]

2.5.2.2. CHARACTERIZATION ON DISSIMILAR WELDS FOR OFFSHORE APPLICATIONS

Dissimilar welding in an offshore application has turned out to be an effective and successful solution that has considerably replaced the earlier sleeve and cathodic protection methods. Various research groups worldwide have been actively involved in identifying new sites for employing dissimilar joints, characterizing the existing joints more comprehensively. All these efforts have been aimed at enhancing the structural integrity of offshore structures. Eghlimi et al., fabricated a GTA weld between super duplex 2507 and austenitic stainless steel 304 using super duplex 2594 filler wire [Eghlimi et al., 2015a]. The authors have conducted a detailed metallurgical investigation using optical, scanning microscopy, EBSD, and texture analysis. The results indicate that weld metal was mostly composed of widmanstatten and grain boundary austenite. The weak texture locations were dominated with low angle boundaries, and the ferrite content increased considerably, whereas a significant reduction in texture intensity was observed. Partial ferritization of weld changed the morphology of microstructure from rolled to twinned PTA placed irregularly between ferrite textured colonies. The authors have also performed similar studies using austenitic filler wire. In this case, the weld metal showed the highest residual strain and had large austenite grain colonies of similar orientations with little amounts of skeletal ferrite [Eghlimi et al., 2015b]. Effect heat input on the properties of super duplex 2507/ API X65 steel was investigated by Sadeghian et al. in a GTA welded joint [Sadeghian et al., 2014]. The welds were fabricated with two different heat inputs: 0.506 and 0.86 kJ/mm. The impact strength at -20°C for the sample with low heat input was found to be lower than the base metal, whereas, for the sample with high heat input, it was higher than the base metal. Although both the welds were devoid of any detrimental intermetallic phases, high heat input lead to a lower amount of ferrite content in the weld zone. Figure 2.17 represents the comparative feature of the welds fabricated at different heat inputs.

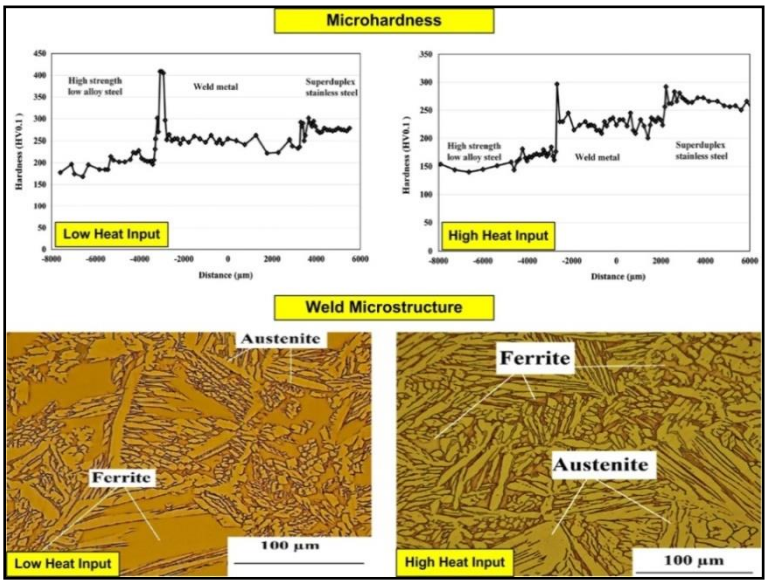

Figure 2.18: Effect of heat input on 2507/X65 GTA weld [Sadeghian et al., 2014]

A dissimilar joint between super duplex and austenitic stainless steel is also widely used in offshore equipment and components. A comparative study of the GTA welds between these two steels fabricated using ER2594 and ER309LMo was carried out using mechanical and microstructural characterizations [Rahmani et al., 2014]. Although both the joints qualified the minimum required values, the impact strength and hardness were comparatively better in the case of ER2594 filler. The 309LMo weld zone had delta ferrite in the skeletal morphology, whereas the ER2594 welds show precipitation of secondary austenite in multiple morphologies

as the cooling of weld proceeds (Figure 2.18). A similar approach of comparing ER2209 and ER309 electrodes for fabricating dissimilar duplex 2205/X52 SMAW joint [Belkessa et al., 2016]. Shielded metal arc welds were fabricated, keeping the weld geometry and process parameters the same for both the electrode types. Results indicate that ER309L electrodes fair better in tensile and impact strength, whereas the corrosion resistance of ER2209 weld was found to be superior. The weld microstructure of the ER 2209 electrode had multiple austenite precipitation, whereas 309L showed just the presence of skeletal ferrites. A comparative representation of weld properties from both the electrodes is shown in Figure 2.19.

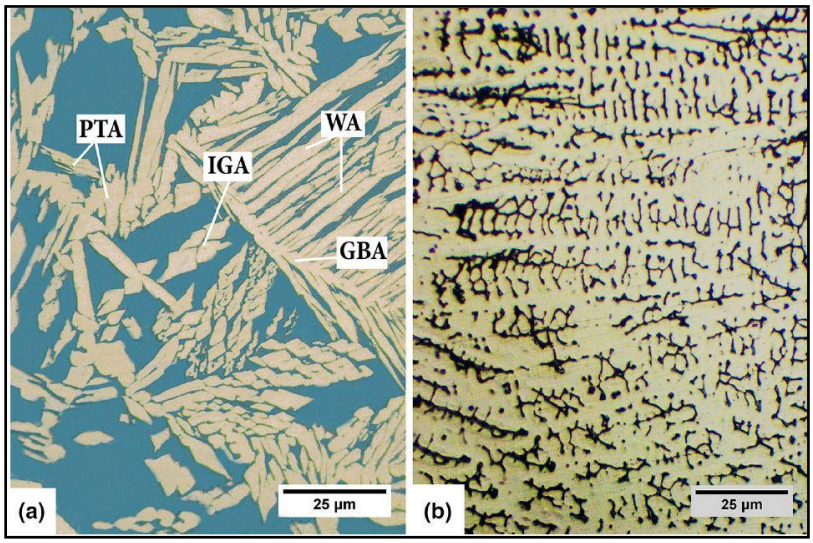

Figure 2.19: GTA weld zone microstructure: (a) ER2594 filler (b) ER309LMo filler [Rahmani et al., 2014]

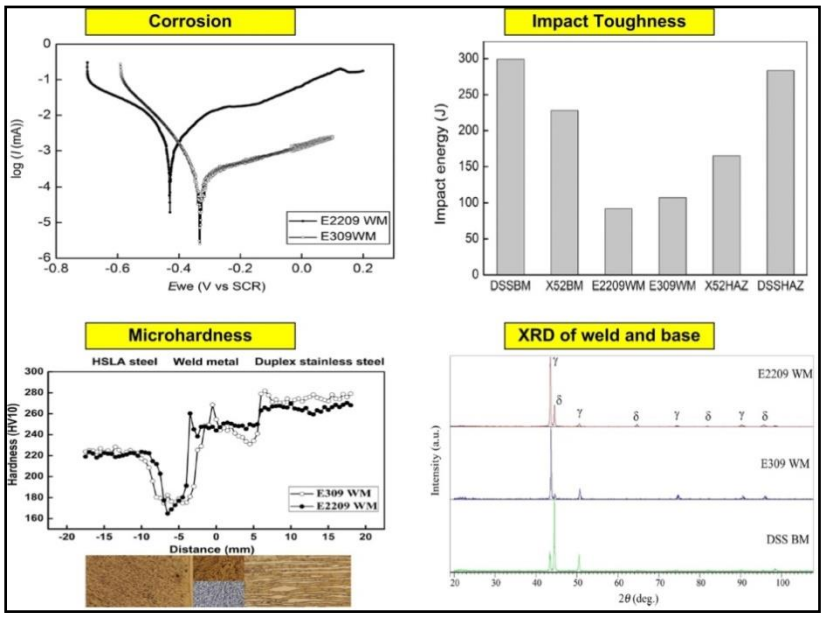

Figure 2.20: Comparison of SMAW 2205/X52 fabricated using ER2209 and ER309L [Belkessa et al., 2016]

Summary of Chapter 2

This chapter presented a comprehensive literature review of different aspects related to the title of this thesis. An attempt has been made to trace the advent of modern offshore structures, followed by the discussion on materials used for marine offshore locations. API pipeline steel, and high corrosion resistant super duplex stainless steels have been discussed in detail, citing the previous studies available on their development, mechanical and microstructural behavior. Need of dissimilar welds has been outlined and two methods; SMAW and GTAW used for weld fabrication have been discussed to give a primary idea. Understanding the importance of consumable in welding procedure, a separate section on SMAW consumable development has been given along with mentioning the characterizations performed on GTAW dissimilar pipeline/super duplex joint with offshore application.